MAPPING ROADSIDE NITROGEN DIOXIDE CONCENTRATIONS USING NON-STATIONARY KRIGING

Serge A. Séguret[1], Laure Malherbe[2*], Gilles Perron[3]

(1) *Centre de Géostatistique, Ecole des Mines de Paris, 35, rue Saint-Honoré, 77300 Fontainebleau, France.*

(2) *Institut National de l'Environnement Industriel et des Risques, INERIS, Parc Technologique ALATA, B. P. N° 2, 60550 Verneuil-en-Halatte, France.*

(3) *Association pour la Surveillance et l'Etude de la Pollution atmosphérique en Alsace, ASPA, 5, rue de Madrid, 67300 Schiltigheim, France.*

Corresponding author. Tel.: +33 3 44 55 62 18; fax: + 33 3 44 55 68 99

E-mail address: laure.malherbe@ineris.fr

Abstract

Atmospheric nitrogen dioxide (NO_2) concentrations around a major road in Alsace (France) are estimated on a fine grid using measurements given by passive samplers and a geostatistical approach. Data are referenced to a local coordinate system where (x, y) are respectively the distance from and along the road. They show a strong non-stationarity which does not allow ordinary kriging to be used in the estimation. Therefore a trend is modelled by a combination of exponential and polynomial functions. Experimental residuals are then computed as the differences between measurements and the trend. The idea is to interpolate the residuals at the nodes of the grid, applying kriging methods, and to add them to the trend estimate. Since their variance is not stationary either, an intermediary step is required. It consists in modelling the standard deviation of the residuals as a function of the drift and normalizing the residuals by this model. This defines a new regionalized variable which can be estimated in the framework of stationary geostatistics. Two possible kriging systems are tested, depending on the fitted variogram model: in the first one, a pure nugget effect (white noise) is used, in which case the best linear estimator of NO_2 concentration is the trend model; in the second one, a structured exponential variogram is adjusted. This case study shows that non-stationarity may not only characterize the raw variable but can

1

31   also affect the variance of a phenomenon. It illustrates the interest of modelling it so as to improve the

32   experimental variogram, fit an acceptable variogram model and compute the variance of the estimation

33   error even if the estimator is reduced to a simple regression function.

34

35   *Keywords*: geostatistics, non-stationarity, trend estimation, standard deviation model, universal kriging

36

37

38   **1. Introduction**

39

40   Air pollution mapping is a valuable tool for assessing population long-term exposure and informing the

41   public about the spatial distribution of outdoor concentrations. At the regulatory level, calculation of

42   concentration maps is prompted by the European daughter directives on ambient air quality assessment

43   (1999/30/ EC, 2000/69/ EC, 2002/3/ EC).

44   In France geostatistical methods have been receiving particular attention for several years and are now

45   commonly used by the French air quality monitoring organizations. They are mostly applied for mapping

46   background concentrations at the city or regional scale so as to fulfill the regulatory recommendations.

47   Roadside pollution is equally a matter of concern as regards people exposure and has been the subject of

48   many investigations (Gilbert, 2003, Kodama, 2001, Roorda-Knape, 1999). However, the difficulty in such

49   cases is that concentration usually shows a strong drift (it decreases with distance from the source), which

50   makes the classical methods of stationary geostatistics like ordinary kriging or cokriging unsuitable.

51   Deletraz and Dabos (2001) tested different interpolating methods in order to map the environmental

52   impact (expressed as NO_2 deposition) of a road in a mountainous region and opted for a multiple

53   regression estimator using the inverse distance from the road and the logarithm of roughness as

54   explicative variables. The regression model explains 87% of the deposition variability. Unlike the

55   geostatistical method explored hereafter, it does not take the residual variability into account. Briggs et al.

56   (2000) also proposed a regression mapping technique to model the spatial patterns of traffic-related

57   pollution. The developed model is a linear combination of variables derived from traffic counts, land

58   cover and altitude.

59   Several studies show the relevance of geostatistics to treat non-stationary problems in the vicinity of

60   chemical or contaminating sources. Figueira et al. (1999) applied kriging with external drift for estimating

61   soil salinity in a coastal land strip. The logarithm of the distance from the coast was used as an auxiliary

62   variable. The results were compared with those of ordinary kriging. They attested the efficiency of the

external drift. Saito and Goovaerts (2001) applied different techniques based on kriging to estimate lead soil concentrations around a former smelter in Dallas. In particular they modelled a trend by a linear combination of log(d) and $\Delta\theta$, d being the distance from the smelter and $\Delta\theta$ the deviation from the main wind direction. Then they worked with residuals obtained from the difference between measurements and the trend estimates.

In this methodology-oriented study we propose to perform kriging of residuals from a global trend model in order to estimate NO_2 roadside concentrations in the Thur Vosges Valley in Alsace, France.

Concentration data are derived from passive diffusion tube measurements performed 3 meters above the ground at 39 sites around a major road, (Fig. 1-A). The aim of the measurement campaign, which took place in summer 2001, was to assess the environmental impact of traffic. Therefore the samplers were located in places supposed to be strictly under the influence of road emissions. Most tubes were positioned on transepts and situated 1 m, 2 m, 50 m, 200 m, 400 m far from the road. Similar measurements were also conducted in winter. However, the present article focuses on summer average concentrations, calculated from 6 fortnightly records. Results for winter are mentioned only if they present significant differences with summer. The road is 20 km long. To simplify its width has been set to zero as it is not precisely known.

Among all the auxiliary variables (land use, emission inventory, population density …) distance to the road and elevation appear to be explanatory of NO_2 concentration, as indicates a Factorial Component Analysis. Now, the elevation is strongly correlated with distance along the road (curvilinear abscissa) (see Fig.1-B). Consequently NO_2 concentrations are expressed in a coordinate system where (x, y) are distances from and along the road, respectively (Fig. 1-C). By this way elevation is implicitly taken into account.

Data show a clear tendency of NO_2 concentration to decrease with distance from the road, indicating the non-stationary nature of the pollution phenomenon. In that context a mapping methodology based on estimating the trend is suggested.

In what follows, concentration measurements are considered as the realization of a random function $NO_2(x,y)$. The estimation involves four stages.

94   1. At any point (x,y), NO$_2$ is written as the sum of a trend m(x,y) providing the general pattern of

95   pollution along and across the road, and a random residual: NO$_2$(x,y)=m(x,y)+R(x,y)

96   Therefore this first step consists in adjusting a trend model on the concentration data.

97   2. As the variance of the residuals depends on their value (non stationary variance), those residuals have

98   to be normalized so that classical kriging methods can be applied. For this purpose their standard

99   deviation is modelled by a function σ(x,y).

100   3. The experimental variogram of the normalized residuals NR(x,y)=R(x,y)/σ(x,y) is calculated to

101   describe the spatial variability of concentration fluctuations around the trend and a variogram model is

102   fitted.

103   4. A simple kriging system is solved to estimate NR(x,y) at the nodes of a 250m x 250m mesh grid.

104   Finally the estimator of NO$_2$(x,y) is built :

$$NO_2^{\,*}(x, y) = \sigma(x, y)NR^{*}(x, y) + m(x, y)$$

105
106   After presenting each stage, we conclude by a discussion where :

107   -   the results are interpreted;

108   -   other possible kriging systems are considered, depending on the confidence given to the trend

109   estimate.

110

111 2. Modelling the trend

112

113   As a preamble, let us define the notion of non-stationarity : a regionalized phenomenon, namely a

114   physical phenomenon stretching out in space and represented by a function Z, is stationary if its mean

115   m(p) and its covariance cov[Z(p),Z(p+h)] are independent of the location of point p.

116   Fig. 2-A represents the projection of concentrations on a plane perpendicular to the road. Two main

117   observations can be made: 1) NO$_2$ concentration decreases sharply with distance from the road, indicating

118   the non-stationary nature of the phenomenon; 2) there is no significant dissymmetry between the left and

119   right sides of the road. The first remark involves trend modelling, the second one allows us to handle the

120   left and right sides together, increasing the total number of available data in a class and hence, the

121   accuracy of the model.

122   A difficult task is now to give a proper analytical form to the trend.

123

124 • For a given y = y_j, i.e. when concentration variations are examined perpendicularly to the road,

125   optimality in the least square sense is obtained in the frame of a bi-exponential function of x :

$$m(x,y_j) = a(y_j)\, e^{-\frac{|x|}{s_1}} + b(y_j)e^{-\frac{|x|}{s_2}}$$ [1]

126 with $(s_1, s_2) = (18, 550)$. For distances from the road greater than 1600 meters the drift can be considered

127 as zero. The average concentrations and their interpolated values by function (1) are represented in Fig. 2-

128 B.

129 In winter $(s_1, s_2) = (14, 940)$. Concentrations are distributed following a different pattern, and become

130 zero at more than 3000 meters from the road. Such a difference with summer can be explained by

131 climatology, changes in the emissions and photochemical consumption of nitrogen oxide in summer.

132 Such observations are consistent with what Monn et al. (1997) already noticed.

133

134 • For a given x = x_i, i.e. when concentration variations are examined parallel to the road, optimality in

135   the least square sense is obtained in the frame of a linear function of y (Fig. 2-C) :

$$m(x_i,y) = c(x_i)\, y + d(x_i)$$ [2]

136

137 • Combining formulas (1) and (2) leads to the trend model :

$$m(x,y) = c_0 + (c_1 y + c_2)\, e^{-\frac{|x|}{s_1}} + (c_3 y + c_4)e^{-\frac{|x|}{s_2}}$$ [3]

138

139 The constant c_0 is introduced so that the trend is not necessarily zero for distances from the road greater

140 than 1600 meters ; the factors s_1 and s_2 are fixed once and for all; the coefficients c_0 to c_4 are obtained by

141 a global regression on the 39 measurements. The trend is represented in three dimensions (Fig. 3-A) and

142 by isovalues (Fig 3-B).

143 Results are different for each season. For exemple, c_0 is equal to 0.3 µg m^{-3} in summer and 3.5 µg m^{-3} in

144 winter.

145

146 Most measurements are located at distances to the road less than 400 meters. Beyond that, the trend

147 model is not conditioned by experimental data and only determined by the mathematical properties of the

148 exponential functions. To prevent improper extrapolation, the use of m(x,y) is restricted to x values below

149 500 meters on both sides of the road ($|x|<500$ m).

150

3. Non-stationarity of the variance

Let u be the coordinate vector (x,y). Using the trend model (3) the residuals R(u) are calculated at the measurement points :

$$R(u) = NO2(u) - m(u) \qquad [4]$$

Those residuals are plotted as a function of m(u) in Fig. 4-A. As expected they fluctuate around 0 but the amplitude of the fluctuations increases with m(u), suggesting that the variance of the residuals is not stationary. Therefore this variance has to be modelled too. The trend values calculated at the sampling points are gathered in six different classes and for each class the standard deviation of the residuals is computed. A power function of m(u) is then adjusted (Fig. 4-B) :

$$\sigma(u) = d\, m(u)^p \qquad [5]$$

The parameters d and p are equal to 0.261 and 0.879 respectively (d=0.015 and p=1.57 in winter).

4. Variograms

To get stationarity the residuals are normalized :

$$NR(u) = \frac{R(u)}{\sigma(u)} \qquad [6]$$

Such an operation is possible because $\sigma(u)$ is strictly positive in the domain under study.

Is this normalization (6) really necessary ? The transverse semivariogram (i.e. perpendicular to the road) of R(u) is plotted in Fig. 5-A : the large fluctuations are mainly explained by the contrast of variability between the measurements close to the road and the other concentration measurements. If the non-stationarity of the variance is ignored and the residuals are not normalized then the variance assigned to the first set of measurements is too low and the variance assigned to the second one is too high. Normalization makes it possible to homogenize residuals and is essential to go further in the analysis.

When calculated on NR(u), the transverse variogram is significantly improved (Fig. 5-B). The longitudinal variogram (i.e. along the road, Fig. 5-C) has a cyclic aspect due to the alternation of higher (about 50 μg m^{-3}) and lower (about 40 μg m^{-3}) values for samplers located at distances less than 2 meters from the road. The housing type may explain such concentration variations but additional information need to be collected to confirm such an hypothesis. The first point of the longitudinal variogram is calculated with only ten pairs of data whereas the second one is computed with 118 pairs. Whether or not

6

178   the first point is taken into account and the transversal or longitudinal variogram is assigned with a

179   structure, two approaches are examined :

180   -   the variogram is considered as not being structured in any of the directions (white noise) : it is

181   modelled by a pure nugget effect equal to the variance of NR(u) : C(0)=1.13.

182   -   a structure is detected and described by the sum of a nugget effect and an exponential model with a

183   geometrical anisotropy of ranges 1450 m in the x-direction and 10000 m in the y –direction

184   (respectively 80 m and 2200 m in winter).

185

186   5. Estimation

187

188   Whatever the approach, let C(h) be the covariance of NR(u). It is linked to the stationary variogram by

189   the relationship :

190      $C(h) = C(0) - \gamma(h)$

191   The normalized residuals are estimated at the nodes $u_0 = (x_0, y_0)$ of a grid by a linear combination of the n

192   = 39 concentration measurements :

$$NR^*(u_0) = \sum_{\alpha=1}^{n} \lambda_\alpha \ NR(u_\alpha) \qquad \text{[7-a]}$$

193   The kriging weights λ_α are the solution of a simple kriging system :

$$\sum_{\alpha=1}^{n} \lambda_\alpha \ C_{\alpha\beta} = C_{\beta 0} \qquad\qquad \forall \beta : 1, n \qquad \text{[7-b]}$$

194   where $C_{\alpha\beta}$ (resp. $C_{\beta 0}$) stands for the covariance between measurements taken in u_α and u_β (resp. u_β and

195   u_0).

196   The estimator of $NO_2(u_0)$ is obtained setting :

$$NO_2^*(u_0) = \sigma(u_0) \ NR^*(u_0) + m(u_0) \qquad \text{[7-c]}$$

197   where $m(u_0)$ and $\sigma(u_0)$ are given by (3) and (5).

198   The variance of the estimation error is :

$$\sigma^2_{NO_2}(u_0) = \sigma^2(u_0) \ (C(0) - \sum_{\alpha=1}^{n} \lambda^\alpha C_{\alpha 0}) \qquad \text{[7-d]}$$

199   When the covariance C(h) is described by a pure nugget effect, the weights minimizing (7-d) are all zero

200   and the estimation is reduced to :

$$NO_2*(u_0) = m(u_0)$$ [8-a]

201 This result is actually well-known : kriging with a nugget covariance is strictly equivalent to estimating

202 the trend. Here the trend has been obtained by a mean-square regression. At each node of the grid, the

203 estimation variance is then :

$$\sigma^2_{NO_2}(u_0) = \sigma^2(u_0)\, C(0)$$ [8-b]

204 As C(0) is close to 1, σ_{NO2} is nearly equal to the non-normalized residues standard deviation model σ

205 given by (5).

206 Fig. 6-A shows the estimation of concentrations using an exponential covariance. Comparing it with the

207 trend representation (Fig. 3-B) makes it evident how the isolines get distorted to fit the experimental

208 values. Such a comparison points up the advantage of kriging over a mean-square regression and the

209 interest of modelling the variogram when possible. The estimation standard deviation for that kriging is

210 displayed in Fig. 6-B. Compared to the one associated with regression (Fig. 6-C) it is lower around the

211 data points.

212

213 **6. Conclusion and discussion**

214

215 Through the analysis of a case example, a methodology is proposed for elaborating concentration maps in

216 presence of a spatial trend. Though the limited number of data did not facilitate the interpretation of the

217 variogram (see section 4), our aim was to point out the interest of modelling non-stationarity when it

218 affects a variable and its variance. Here we discuss the choices we made for calculating the variogram and

219 defining a model.

220

221 **6.1   Interpretation of the results**

222 The variogram $\gamma(h)$ is computed with residuals derived from a trend estimate, which necessarily

223 introduces a bias (Matheron, 1970). As a consequence, the real underlying variogram, assuming it is

224 structured, can be either masked or deformed, depending on the representativity of the data. Quantifying

225 the impact of the number of samplers on the quality of the trend estimate is not easy. However the

226 estimation standard deviation map for a nugget covariance model may be a useful tool for evaluating

227 kriging results (Fig. 6-C). On the road axis the standard deviation is 8 μgm^{-3} at y=5 km. Then it decreases

228 sharply till it reaches 1 at y = 20 km and x = ±500m. If the standard deviation is not to be larger than 3.5

229 μgm^{-3} for example, then only the area where this condition is met should be selected for representing

230 concentrations, whereas estimates near the road are ignored (hatched region in Fig. 6-C). This

231 interpretation of the kriging standard deviation map is strengthened by sensitivity tests consisting in

232 estimating m(x, y) with restricted data sets. According to such tests, the trend estimate was sensitive to

233 data located less than 2 m from the road. For longer distances the coefficients c_0 to c_4 of formula (3) did

234 not change significantly if 4 or 5 measurements were removed randomly. The poorer quality of estimation

235 near the road is to be expected since concentrations, and hence the estimation variances, are higher there.

236 To improve it, more measurements are required.

237

238 The kriging standard deviation map for an exponential covariance model (Fig. 6-B) can be studied in the

239 same way. Regions respecting the quality criterion, expressed as a maximal value for kriging standard

240 deviation, can be selected as previously.

241

242 **6.2   Using the IRF-k theory ?**

243 A drawback of the proposed methodology is that the final NO_2 concentration estimate closely depends on

244 the mean-square trend estimate. To weaken this dependency relationship a more elaborated kriging

245 system might be used. Actually two different systems could be envisaged :

246   -   universal kriging of NO_2 (Appendix 1) : an affine function of the trend m(u) is reestimated;

247   -   a more general universal kriging of NO_2 (Appendix 2): all the coefficients of the trend are

248   reestimated.

249 Whatever the chosen method, all the systems proceed from the non stationary approach called Universal

250 Kriging (Matheron, 1969) and do not solve the problem of the bias of the variogram which has been

251 previously mentioned.

252 The theory of the Intrinsic Random Functions of order k (IRF-k) (Matheron, 1971) was developed to

253 answer that problem. A synthetic description can be found in Chilès and Delfiner (1999). To summarize,

254 we can say that this theory implies fitting most part of the phenomenon by all possible linear combination

255 of polynomials having a given degree k, the variability of the residuals being modelled by a Generalized

256 Covariance. This method is useful when polynomials can explain the large-scale spatial behaviour of the

257 phenomenon under study. Is it the case here? Fig. 7 represents the averaged concentrations projected on a

258 plane perpendicular to the road, and their regression by polynomials. To obtain an acceptable

259 approximation, we need to use at least all the degrees of x up to 4. This implies modelling the trend using

260 a term in yx^4 relevant of an IRF-5. As the set of polynomials must be complete, in order to ensure the

261 regularity of the kriging system, the trend must then be developed on 21 monomials with as much

262 multiplicative coefficients to be calculated. This is not reasonable.

263

264 Universal kriging seems therefore to be an effective way of handling the problem of double non-

265 stationarity in mean and variance. It is based on hypotheses consistent with the spatial pollution pattern.

266 Besides this methodology does not involve complex mathematical developments and is suitable for

267 regular use, in compliance with regulatory requirements.

268

269 **Appendix 1 : Universal Kriging of NO_2**

270 A linear system is built where a linear function of the trend m(u) is locally estimated by kriging. $NO_2(u)$

271 is consequently expressed as :

$$NO_2(u) = \sigma(u)\ NR(u) + a_0\ m(u) + a_1 \qquad\qquad [A1\text{-}1]$$

272 where a_0 and a_1 are unknown and m(u) is the trend previously obtained by least square regression. The

273 specificity of the present application is a non stationary covariance :

$$Cov(NO_2(u), NO_2(v)) = \sigma(u)\ \sigma(v)\ C(v\text{-}u) \qquad\qquad [A1\text{-}2]$$

274

275 At any node u_0 of the estimation grid, the estimator is a linear combination of measurements taken at the

276 points u_α :

$$NO_2{}^*(u_0) = \sum_{\alpha=1}^{n} \lambda_\alpha\ NO_2(u_\alpha) \qquad\qquad [A1\text{-}3]$$

277 The weights λ_α are solutions of the following system :

$$\sum_{\alpha=1}^{n} \lambda_\alpha \sigma(u_\alpha)\ \sigma(u_\beta)\ C_{\alpha\beta} + \mu_0 + \mu_1\ m(u_\beta) = \sigma(u_\beta)\ \sigma(u_0)\ C_{\beta 0} \qquad \forall \beta : 1, n \qquad [A1\text{-}4]$$

$$\sum_{\alpha=1}^{n} \lambda_\alpha = 1 \qquad\qquad [A1\text{-}5]$$

$$\sum_{\alpha=1}^{n} \lambda_\alpha m(u_\alpha) = m(u_0) \qquad\qquad [A1\text{-}6]$$

278 The estimation error is defined as the difference $NO_2{}^*(u_0)\text{-}NO_2(u_0)$. Its variance is given by :

$$\sigma_{NO_2}^2(u_0) = \sigma^2(u_0)\ C(0) - \sum_{\alpha=1}^{n} \lambda^\alpha \sigma(u_\alpha)\ \sigma(u_0)\ C_{\alpha 0} - \mu_0 - \mu_1\ m(u_0) \qquad [A1\text{-}7]$$

279 Coefficients μ_0 et μ_1 are Lagrange parameters imposed by the universality conditions (A1-5) and (A1-6).

280 Equations (A1-4) to (A1-6) make a classical Universal Kriging system which has the distinctive feature of

281 using a non-stationary covariance $\sigma(u)\sigma(u+h)C(h)$. This system is reversible and has a unique solution

282 since the covariance $\sigma(u)\sigma(u+h)C(h)$ is positive definite like $C(h)$. The data are NO_2 measurements (and

283 not the normalized residuals NR). It must be useful to use a moving neighborhood with at least 10

284 measurements around the node u_0 where the estimator is calculated.

285

286 **Appendix 2 : more general Universal Kriging of NO_2**

287 A linear system is built where the coefficients c_0 to c_4 of the trend $m(u)$ are locally estimated by kriging.

288   If we put :

289 $\{X^l, 1=1 \text{ to } 5\} = \{1,\ e^{-\frac{|x|}{s_1}},\ e^{-\frac{|x|}{s_2}},\ y\,e^{-\frac{|x|}{s_1}},\ y\,e^{-\frac{|x|}{s_2}}\}$

290 the kriging system becomes :

$$\sum_{\alpha=1}^{n}\lambda_\alpha\sigma(u_\alpha)\,\sigma(u_\beta)\,C_{\alpha\beta} + \sum_{l=1}^{5}\mu_l X^l(u_\beta) = \sigma(u_\beta)\,\sigma(u_0)\,C_{\beta 0} \qquad \forall \beta : 1, n \qquad [A2\text{-}1]$$

$$\sum_{\alpha=1}^{n}\lambda_\alpha X^l(u_\alpha) = X^l(u_0) \qquad\qquad \forall\, 1 : 1, 5 \qquad [A2\text{-}2]$$

291 and the variance of the error is :

$$\sigma^2_{NO_2}(u_0) = \sigma^2(u_0)\,C(0) - \sum_{\alpha=1}^{n}\lambda^\alpha\sigma(u_\alpha)\,\sigma(u_0)\,C_{\alpha 0} - \sum_{l=1}^{5}\mu_l\,X^l(u_0) \qquad [A2\text{-}2]$$

292 Those expressions use five Lagrange multipliers μ_l. As previously, it is advised to use a moving

293 neighborhood. The selected data must not lie on a line.

294

303

References

304 **References**

305 Briggs, D.J., Hoogh (de), C., Gulliver, J., Wills, J., Elliott, P., Kingham, S., Smallbone, K., 2000. A

306 regression-based method for mapping traffic-related air pollution: application and testing in four

307 contrasting urban environments. The Science of the Total Environment, 253, 151-167.

308

309 Chilès, J.-P., Delfiner, P. 1999. Geostatistics. Modeling Spatial Uncertainty. Wiley, New York.

310

311 Deletraz, G., Dabos, P. 2001. Modélisation statistique de la pollution azotée à proximité d'un axe routier

312 et évaluation des incidences sur l'environnement. Colloque Risques – octobre 2001, Besançon.

313

314 Council Directive 1999/30/EC of 22 April 1999 relating to limit values for sulphur dioxide, nitrogen

315 dioxide and oxides of nitrogen, particulate matter and lead in ambient air.

316

317 Directive 2000/69/EC of the European Parliament and of the Council of 16 November 2000 relating to

318 limit values for benzene and carbon monoxide in ambient air.

319

320 Directive 2002/3/EC of the European Parliament and of the Council of 12 February 2002 relating to

321 ozone in ambient air.

322

323 Figueira, R., Sousa, A.J., Pacheco, A.M.G., Catarino, F. 1999. Saline variability at ground level after

324 kriging data from *Ramalina* app. Biomonitors. The Science of the Total Environment, 232, 3-11.

325

326 Gilbert, N.L., Woodhouse, S., Stieb, D.M., Brook, J.R., 2003. Ambient nitrogen dioxide and distance

327 from a major highway. The Science of the Total Environment, 312, 43-46.

328

329 Kodama, Y., Arashidani, K., Tokui, N., Kawamoto, T., Matsuno, K., Kunugita, N., Minakawa, N., 2002.

330 Environmental NO_2 concentration and exposure in daily life along main roads in Tokyo. Environmental

331 Research, Section A, 89, 236-244.

332

333 Matheron, G., 1969. Le Krigeage Universel. Cahiers du Centre de Morphologie Mathématique de

334 Fontainebleau, Fascicule 1, Ecole des Mines de Paris.

335

336   Matheron, G. 1970. La Théorie des Variables Régionalisées et ses Applications. Cahiers du Centre de

337   Morphologie Mathématique de Fontainebleau, Fasc. 5, Ecole des Mines de Paris. Translation (1971) :

338   The Theory of Regionalized Variables and Its applications.

339

340   Matheron, G. 1971. La Théorie des Fonctions Aléatoires Intrinsèques Généralisées. Note Géostatistique

341   No 117. Technical Report N-252, Centre de Géostatistique, Fontainebleau, France.

342

343   Monn, Ch., Carabias, V., Junker, M., Waeber, R., Karrer, M., Wanner, H.U. 1997. Small-scale spatial

344   variability of particulate matter <10 μm (PM_{10}) and nitrogen dioxide. Atmospheric Environment, 31 (15),

345   2243-2247.

346

347   Roorda-Knape, M., Janssen, N.A.H., Hartog (de), J., Van Vliet, P.H.N., Harssema, H., Brunekreef, B.,

348   1999. Traffic related air pollution in city districts near motorways, The Science of the Total Environment,

349   235, 339-341.

350

351   Saito, H., Goovaerts, P., 2001. Accounting for source location and transport direction into geostatistical

352   prediction of contaminants. Environmental Science and Technology, 35, 4823-4829.

353

354   Séguret, S.A., 2003. Estimation du dioxyde d'azote routier dans la vallée de la Thur. Technical Report N-

355   1/03/G   available   on   pdf   file   at   http://www.lcsqa.org.

Figure captions

357

358 Fig. 1 : (A) Road representation in the original geographical system. The red points stand for the 39

359 measurement points, 33 of which lie on transepts T1 to T6.

360 (B) Correlation cloud between altitude and measurement distance along the road (curvilinear abscissa).

361 (C) Location of measurements in the local reference system.

362

363

364 Fig. 2 : (A) Projection of the measurement data onto a plane perpendicular to the road (only data located

365 on transepts have been projected). Black points represent the average concentrations for different distance

366 classes ($|x|$=1m, 2m, 50m, 200m and 400m apart from the road).

367 (B) Average concentrations for the considered distance classes and adjustment of a combination of two

368 exponential functions.

369 (C) Concentration variations along the road (i.e. along y) for each $|x|$-distance class and their

370 approximation by linear functions.

371

372

373 Fig. 3 : (A, B) Graphic representation of the trend m(x,y) in perspective (A) and in isolines (B). The red

374 and black isolines are 10 µg m^{-3}and 2 µg m^{-3} distant from each other, respectively.

375

376

377 Fig. 4 : (A) Residuals R(u) = NO$_2$(u) - m(u) as a function of the trend m(u). u = (x,y) is the coordinate

378 vector in the local reference frame. R(u) fluctuations around 0 grow with m(u). (B) R(u) standard

379 deviations for each m(u) value class and adjustment of a model written as d m(u)^p, with d=0.261 and

380 p=0.879.

381

382

383 Fig. 5 : (A) Experimental variogram of the residuals R(u) in the transverse direction before

384 standardization. (B) Experimental variogram of the standardized residuals R(u) in the transverse

385 direction. The number of pairs participating to the calculation of each point are indicated on the graph.

386 Two types of models have been fitted: a pure nugget model (in blue) and a nugget+exponential

387   anisotropic model with a range of 1.45 km along x and 10 km along y. (C) Variogram of the standardized

388   residuals along the road.

389

390

391   Fig. 6 : (A) Nitrogen dioxide concentration obtained by simple kriging of the standardized residuals,

392   using a structured variogram model. Size of the data points is proportional to the measurement values. (B)

393   Kriging standard deviation for the above calculated map. (C) Kriging standard deviation for a pure nugget

394   variogram model. It is almost equal to $\sigma(x,y)$ and can be regarded as the error standard deviation for the

395   trend estimation. In the red hatched area the standard deviation is greater than 3.5.

396

397

398   Fig. 7 : NO_2 concentrations across the road (green dashed curve) and their approximation by 2nd to 4th

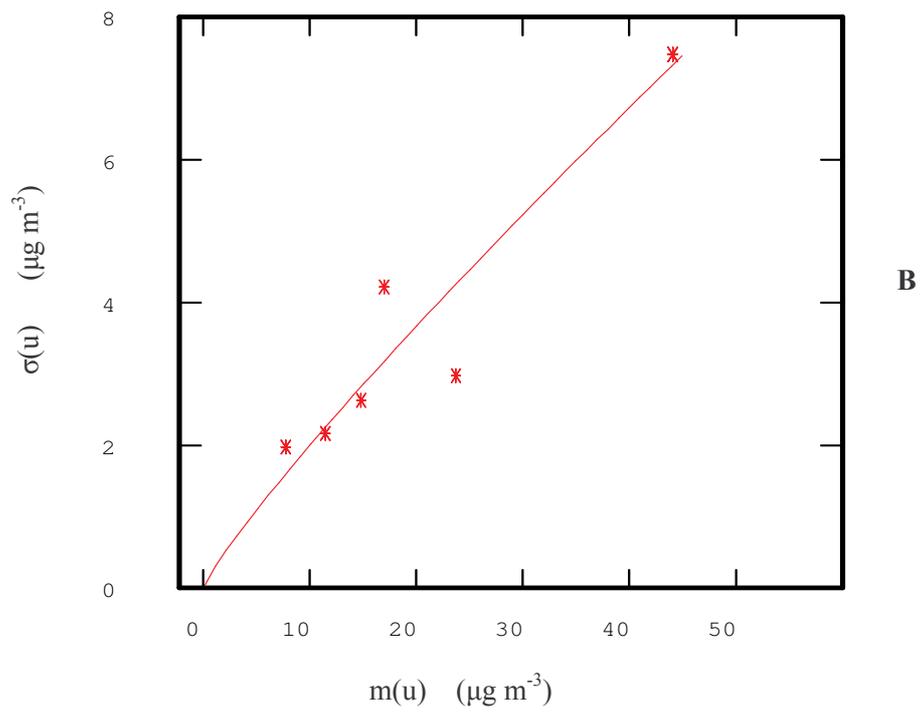399   order polynomial functions (solid curves).

400

401   **Colour illustrations**

402

A

403

404   Fig. 1

405

406
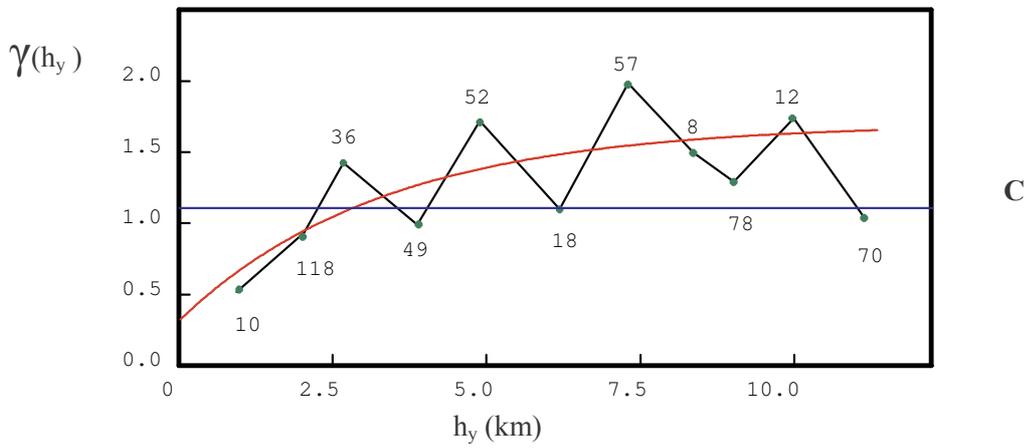
407

408

409   Fig. 2

410

A

B

y : distance along the road (km)

411   Fig. 3

412

413   Fig. 4

414

A

γ(h_x)

B

Model 1

C

415   Fig. 5

416

20

417   Fig. 6

418

μg m⁻

NO2(x, y=y$_j$)

Degree 4 of x

Degree 3 of x

Degree 2 of x

x : distance to the road

419   Fig. 7

420